Article published online: 2025-01-08

An Unusual Observation in Metastatic Neuroendocrine Neoplasm: Diffuse Pattern Hepatic [^{68}Ga]Ga-DOTATATE Uptake Related to Micro-metastatic Disease and Discordance between Dual-Tracer PET-CT Findings and MIB-1 Labelling Index

Parth Baberwal[1,2] Sunita N. Sonavane[1,2] Sandip Basu[1,2]

[1] Radiation Medicine Centre, Bhabha Atomic Research Centre, Tata Memorial Hospital Annexe, Mumbai, Maharashtra, India
[2] Homi Bhabha National Institute, Mumbai, Maharashtra, India

Address for correspondence Sandip Basu, MBBS (Hons), DRM, Diplomate NB, MNAMS, Radiation Medicine Centre (BARC), Tata Memorial Hospital Annexe, Jerbai Wadia Road, Parel, Mumbai, Maharashtra 400012, India (e-mail: drsanb@yahoo.com).

World J Nuclear Med

Abstract

Neuroendocrine neoplasms (NENs) are a rare and diverse group of neoplasms that can originate from neuroendocrine cells in any organ. We herein present a patient with Grade II neuroendocrine tumor (NET) of the pancreas with bilobar liver metastasis and a MIB-1 labelling index of 15%, who underwent various systemic and targeted therapies. On follow-up, dual-tracer PET-CT imaging with [^{68}Ga]Ga-DOTATATE PET/CT showed new onset skeletal metastases and diffuse pattern SSTR (somatostatin receptor) expression in the left lobe of the liver (Krenning score 3), contrasted by absent uptake on [^{18}F]FDG. Magnetic resonance imaging of the liver confirmed sub-centimetric left liver lobe lesions, further biopsy of which suggested Grade-III NET exhibiting high Ki-67 (55–60%). Thus, a discordance was observed between Ki-67 and the dual-tracer PET-CT findings, emphasizing the complexity of NEN imaging (with possibility of differentiation even in a relatively high Ki-67) and the importance of using multiple tracers for accurate assessment in guiding evidence-based management strategy.

Keywords
- metastasis
- NET
- DOTATATE
- FDG
- PET
- discordance
- de-differentiation
- dual-tracer PET

Introduction

Neuroendocrine neoplasms (NENs) are a varied set of tumors that develop from neuroendocrine cells and have different clinical outcomes and presentations.[1] Functional imaging is a pivotal component for diagnosing, staging, and managing neuroendocrine tumors (NETs).[2] Using dual-tracer positron emission tomography/computed tomography (PET/CT) imaging with [^{68}Ga]Ga-DOTATATE and [^{18}F]FDG is especially useful for identifying different characteristics of tumors and guide treatment approaches.[3] This report details a patient with Grade II NET with 15% MIB-1 labeling index at presentation, who initially underwent various systemic and targeted therapies. Follow-up revealed disease progression and inverse discordance between pathology and dual-tracer PET-CT imaging, highlighting the complexity of NET imaging and the necessity of using multiple tracers for accurate assessment in correlation with detailed histopathology, which is crucial for guiding an evidence-based management strategy.

Case Report

A 42-year-old male with a history of diabetes and a family history of undiagnosed malignancy in his mother and grandmother presented with abdominal pain. Diagnostic evaluation revealed a lesion in the tail of the pancreas with multiple bilobar liver metastases. A biopsy of a liver lesion confirmed a

DOI https://doi.org/10.1055/s-0044-1801384.
ISSN 1450-1147.

Thieme Medical and Scientific Publishers Pvt. Ltd., A-12, 2nd Floor, Sector 2, Noida-201301 UP, India

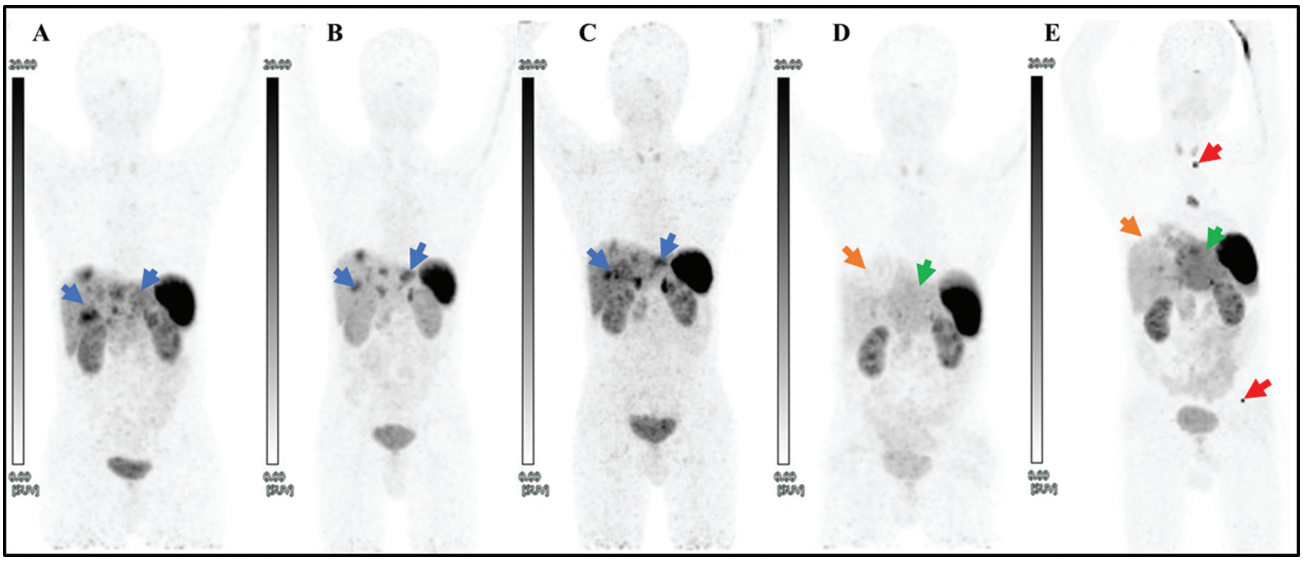

Fig. 1 A series of maximum intensity projection (MIP) images of [^{68}Ga]Ga-DOTATATE PET/CT scan done at baseline (**A**), post 4 cycles of PRRT and 12 cycles of CAPTEM (4 prior to PRRT and 8 cycles sandwiched with PRRT) (**B**), post-CAPTEM and PRRT follow-up (**C**), post 5 cycles of TACE (**D**) and recent follow-up (**E**) showing bilobar liver metastasis (blue arrow) initially responding to systemic therapy; an area of photopenia in right upper aspect of liver post-TACE (orange arrow); heterogeneous diffuse left lobe tracer uptake (more than the normal uptake in the right lobe) that was observed in recent follow-up (E) and retrospectively noted in post-TACE scan (D) as well (green arrow); new-onset SSTR-expressing skeletal metastasis (red arrow) and solitary subcarinal lymphadenopathy. CAPTEM, capecitabine-temozolomide; PRRT, peptide receptor radionuclide therapy.

Grade II NET with an MIB-1 labeling index of 15%. Dual-tracer PET-CT imaging was performed, [^{68}Ga]Ga-DOTATATE--PET/CT showed a somatostatin receptor (SSTR)-expressing lesion in the tail of pancreas (SUVmax: 8.45) and multiple SSTR-expressing bilobar liver lesions (SUVmax: 12.38). [^{18}F] FDG-PET/CT for further disease characterization demonstrated multiple hypodense liver lesions, few of them showing increased metabolism, largest in segment II, measuring 7.1 × 4.7 × 5.6 cm (SUVmax: 11.40), while the primary pancreatic lesion was ametabolic.

The patient underwent 4 cycles of peptide receptor radionuclide therapy (►**Fig. 1A–C**), 12 cycles of capecitabine-temozolomide (CAPTEM), and 4 cycles of trans-arterial chemoembolization (TACE). At the end of treatment (EOT), serum chromogranin A levels were 3,064 mcg/L, and the patient reported clinical improvement. EOT [^{68}Ga]Ga-DOTATATE PET/CT indicated stable disease with TACE-related changes in the right lobe of the liver (►**Fig. 1D**).

At the last follow-up, approximately 1 year later, the patient reported new onset of abdominal and lower back pain. Follow-up dual-tracer PET-CT imaging revealed new SSTR-expressing bilobar liver lesions, SSTR-expressing subcarinal lymph nodes, and SSTR-expressing lytic lesions in the body of the D2 vertebra and left iliac bone (►**Figs. 1E** and **2A**). Additionally, there was diffusely increased SSTR expression (SUVmax: 9.2, Krenning score: 3) in the entire left lobe of the liver, with no definite focal uptake delineated on [^{68}Ga]Ga-DOTATATE (►**Figs. 1E**, **2A**, and **2C**). [^{18}F]FDG-PET/CT revealed new hypermetabolic lesions in the right lobe of the liver (segment V/VI, measuring 3.9 × 1.6 cm with SUVmax of 7.70), a low metabolic subcarinal node (measuring 1.7 × 1.5 cm with SUVmax of 6.13), and minimal [^{18}F]FDG uptake in a few marrow lesions involving the D2 vertebra (SUVmax: 3.75) and left iliac bone (►**Fig. 2B**). Magnetic resonance imaging (MRI) showed new T2-enhancing lesions in both liver lobes with diffusion restriction. The T2 hyperintense enhancing lesions in the left lobe of the liver were multiple and subcentimeter in size (►**Fig. 2E, F**). Serum chromogranin A at this time was >9,000 mcg/L. A biopsy of the left lobe of liver revealed metastatic NET with a mitotic count of 12/10 hpf and no necrosis. Immunohistochemistry showed the tumor cells were diffusely positive for synaptophysin and chromogranin, negative for p40, and focally positive for somatostatin in approximately 5% of tumor cells. The MIB-1 labeling index was 55 to 60% in the most proliferative area. The patient is currently alive and continues to receive treatment from a multidisciplinary team for ongoing management.

Discussion

Histologically, NENs are classified into well-differentiated NETs and poorly differentiated neuroendocrine carcinomas.[4] The MIB-1 index gauges the aggressiveness of tumors.[5] Elevated MIB-1 values reflect increased cell proliferation, suggesting a more aggressive tumor and a poorer prognosis.[6] The MIB-1/Ki-67 index continues to be fundamental in guiding the planning of oncologic therapies.[7] Tumors with higher proliferation indices necessitate more aggressive treatment approaches.[8] The most common site of NENs is the gastrointestinal tract, predominantly mid-gut, followed by lung.[9,10] NETs, on a molecular level, express SSTR, thus, targeted diagnostic and therapeutic approaches can be considered for management. NETs vary a lot in the extent and pattern of the metastasis.[11] In gastroenteropancreatic NETs, the most common site of metastasis is liver.[12] There have been reports of micro-metastatic pattern of disease in case of NETs.[13,14] D'Souza et al detected micro-metastatic disease

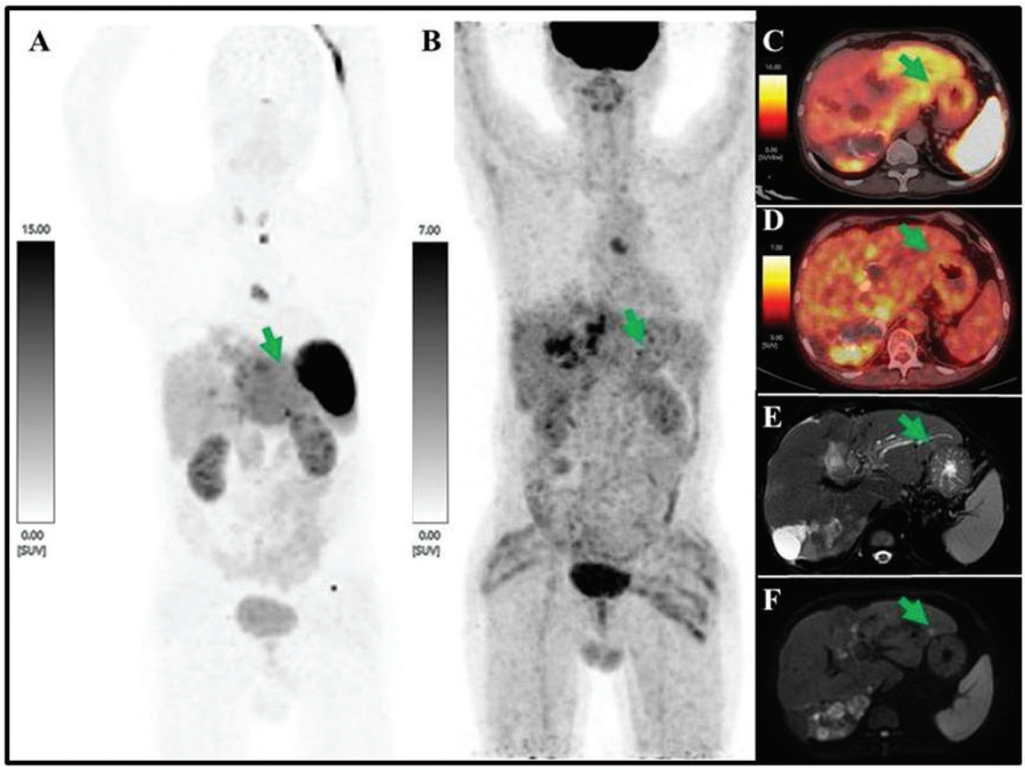

Fig. 2 A MIP of [^{68}Ga]Ga-DOTATATE-PET/CT (**A**) showing heterogeneously diffuse tracer uptake in left lobe of liver (Krenning score 3) while MIP of [^{18}F]FDG-PET (**B**) is showing no correlative tracer uptake concentration. Fused axial view of [^{68}Ga]Ga-DOTATATE-PET/CT (**C**) and [^{18}F]FDG-PET/CT (**D**) showing similar findings as mentioned above. T2-weighted SPAIR (spectral attenuated inversion recovery) MRI axial view (**E**) showing T2 hyperintense enhancing multiple subcentimeter-sized left lobe of liver lesions and axial view of diffusion-weighted MRI (**F**) showing diffusion restriction in the same lesions (marked with green arrow). MIP, maximum intensity projection; MRI, magnetic resonance imaging.

initially with the help of SSTR-PET imaging, where it showed diffusely increased heterogeneous uptake which was more than splenic parenchyma.[14] Albeit liver concentrates [^{68}Ga]Ga-DOTATATE physiologically as well, in our case micrometastases were suspected as left lobe of liver was concentrating [^{68}Ga]Ga-DOTATATE more intensely and diffusely than that of right lobe and uptake had increased significantly in comparison to previous PET/CT, and MRI showed several distinct sub-centimeter-sized metastatic liver lesions in the left lobe.

De-differentiation in NEN though an uncommon phenomenon is a possibility, wherein an increased aggressive profile in metastasis, especially in NETs, can be observed.[15] Less differentiated NENs demonstrate [^{18}F]FDG avidity secondary to high proliferative activity.[16] In our case, however, there was no significant focal/diffuse [^{18}F]FDG avidity in the left lobe of liver, while the histopathology report suggested grade of NET changed to grade III with the reported MIB-1 index increased to 55 to 60%. Thus, dual-tracer imaging with both SSTR- and [^{18}F]FDG PET/CT not only aided in visualizing lesions with different biology, but also harbored prognostic implications.

Conclusion

We present a rare intriguing case of NET of tail of pancreas with liver, nodal, and skeletal metastasis post systemic and targeted therapies presenting with new-onset diffuse left lobe of liver SSTR expression on SSTR-based PET (and negligible uptake on FDG), which on biopsy suggested a relatively de-differentiated metastasis (initial MIB-1 of 15% progressing to 55–60%). This implies that the relation between MIB-1, de-differentiation, and [^{68}Ga]Ga-DOTATATE/[^{18}F]FDG avidity is yet to be completely explored.

Conflict of Interest

None declared.

References

1 Raphael MJ, Chan DL, Law C, Singh S. Principles of diagnosis and management of neuroendocrine tumours. CMAJ 2017;189(10): e398–e404
2 Sadowski S, Reddy S. The role of imaging in neuroendocrine tumors. J Nucl Med 2023;64(01):12–25
3 Sharma P, Qian Y, He M, et al. Dual-tracer PET/CT in neuroendocrine tumors: applications and implications. Cancer Imaging 2023;23(01):5–15
4 Sultana Q, Kar J, Verma A, et al. A comprehensive review on neuroendocrine neoplasms: presentation, pathophysiology and management. J Clin Med 2023;12(15):5138
5 American Cancer Society. Tumor Grade. Accessed August 2, 2024 at: https://www.cancer.org/treatment/understanding-your-diagnosis/staging.html
6 Scholzen T, Gerdes J. The Ki-67 protein: from the known and the unknown. J Cell Physiol 2000;182(03):311–322
7 Dowsett M, Nielsen TO, A'Hern R, et al; International Ki-67 in Breast Cancer Working Group. Assessment of Ki67 in breast cancer: recommendations from the International Ki67 in Breast Cancer working group. J Natl Cancer Inst 2011;103(22):1656–1664

8 Luporsi E, André F, Spyratos F, et al. Ki-67: level of evidence and methodological considerations for its role in the clinical management of breast cancer: analytical and critical review. Breast Cancer Res Treat 2012;132(03):895–915
9 Rothenstein J, Cleary SP, Pond GR, et al. Neuroendocrine tumors of the gastrointestinal tract: a decade of experience at the Princess Margaret Hospital. Am J Clin Oncol 2008;31(01):64–70
10 Silveira F, Basile ML, Kuga FS, Próspero JD, Paes RAP, Bernardi FDC. Neuroendocrine tumors: an epidemiological study of 250 cases at a tertiary hospital. Rev Assoc Med Bras (1002) 2007;63(10): 856–861
11 Cives M, Strosberg JR. Gastroenteropancreatic neuroendocrine tumors. CA Cancer J Clin 2018;68(06):471–487
12 Riihimäki M, Hemminki A, Sundquist K, Sundquist J, Hemminki K. The epidemiology of metastases in neuroendocrine tumors. Int J Cancer 2016;139(12):2679–2686
13 Fazio N, Di Meglio G, Lorizzo K, de Brand F. Miliary hepatic metastases from neuroendocrine carcinoma. Dig Surg 2008;25 (05):330
14 D'Souza JC, O'Brien SR, Yang Z, El Jack AK, Pantel AR. Widespread micronodular hepatic metastases of neuroendocrine tumor detected by [^{68}Ga]DOTATATE PET/CT. Radiol Case Rep 2022;18 (02):481–485
15 Poiană C, Neamțu MC, Avramescu ET, et al. The dedifferentiation of neuroendocrine tumor metastases: myth or reality? Rom J Morphol Embryol 2013;54(01):201–203
16 Adams S, Baum R, Rink T, Schumm-Dräger PM, Usadel KH, Hör G. Limited value of fluorine-18 fluorodeoxyglucose positron emission tomography for the imaging of neuroendocrine tumours. Eur J Nucl Med 1998;25(01):79–83

